JOURNAL OF NANO- AND ELECTRONIC PHYSICS
Vol. **7** No 4, 04011(6pp) (2015)

ЖУРНАЛ НАНО- ТА ЕЛЕКТРОННОЇ ФІЗИКИ
Том **7** № 4, 04011(6cc) (2015)

Variation in Feed Point within Differed L-Slot Multi-frequency Microstrip Patch

Sandeep Arya, Ramni Gupta, Saleem Khan, Parveen Lehana

Department of Physics & Electronics, University of Jammu, J&K, India-180006

(Received 21 July 2015; published online 10 December 2015)

A rectangular microstrip patch antenna with differed pair of L-slots is presented. The proposed antenna is designed to evaluate the effect of alteration in probe-feed point. The proposed microstrip antenna is suitable for bluetooth, mobile and wireless communication applications simultaneously. It is designed successfully for mobile communication systems and Wireless Local Area Networks (WLAN) applications. The results obtained had showed better improvement in the return loss and radiation pattern in comparison to the other existing antennas.

Keywords: Microstrip patch antenna, Multi-frequency actions, L-slots, Probe feeding, Insertion loss, Radiation pattern.

PACS numbers: 84.40.Ba, 95.85.Bh

1. INTRODUCTION

The directivity and the muliti-band integrated antenna configuration generally employ printed circuits and the parameters of the configured antenna depend on the materials employed and their thickness [1]. Due to tremendous increase in the demand of wireless communication devices, it is advantageous to have an integrated antenna that concurrently covers different frequencies/bands for different applications [2-7]. For mobile applications, an integrated antenna is required to simultaneously provide access for GSM (0.9 GHz-1.80 GHz), CDMA (1.90 GHz-2.20 GHz), Bluetooth (2.45 GHz-2.55 GHz) and WiMAX (2.50 GHz-2.70 GHz) while neglecting other frequencies [8]. Moreover, the devices for 3G mobile communication systems must be compatible with 2G. During recent times, several researchers proposed new designs of antennas to be operated in dual and triple band frequencies [9] [10]. There are mainly two feeding methods in a microstrip patch antenna. Feeding RF power directly to the radiating element through a microstrip line or probe feed, known as contacting method. In the non-contacting method, an electromagnetic field coupling is done to transfer power between the microstrip line and the radiating pact that includes proximity feeding and aperture feeding. Thus, there is no physical contact between the elements [11] [12].

In the present work, we have presented the design and the results of the tests of a rectangular microstrip patch antenna. Two differed L-slots are cut in the patch. Probe feeding method is used and the position of the feed point is optimized according to the theoretical analysis. The antenna is then analysed in accordance to the designed dimensions. The paper is planned in a way that details on the analysis of the microstrip patch antenna are given in the Analysis section, whereas the design of the proposed antenna is discussed in the section named Experimental Design. Further, the designed antenna is evaluated for results in the form of output parameters. Results from the tests performed are given in the section Results and Discussions. Finally Conclusions of the work are given.

2. ANALYSIS

In a microstrip patch antenna, the patch behaves as a resonant cavity (short circuit walls on top and bottom, open-circuit walls on the sides), that only allows certain modes to exist at different resonant frequencies, thus, producing significant radiations. For thin substrates, conductor and dielectric losses are prominent while for relatively thicker substrates, surface-wave losses are high. For a thin substrate, the electric field vector is independent of the substrate thickness [13]. The magnetic field inside the patch is given by the Maxwell's equation

$$\vec{H} = -\frac{1}{j\omega\mu}\nabla\times\vec{E} \qquad \text{(i)}$$

Since the area of the patch is spread over the two axes, that is, x-axis and y-axis, and the magnetic field is purely horizontal. Thus, it is assumed that the wave is propagating in the z-direction.

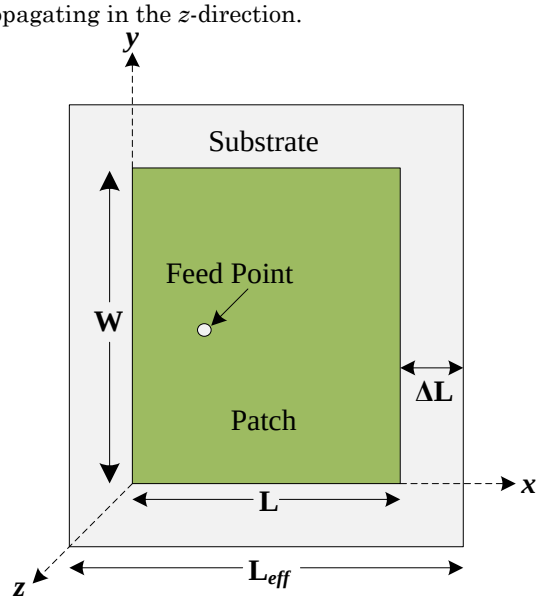

Fig. 1 – Top view of a rectangular microstrip patch antenna

Considering Fig. 1 as the reference for calculations,

the resonance frequency can be calculated by approximating the equations of rectangular wave guide for TM_{mn} mode and the equation is given as

$$\Delta^2 E_z + k^2 E_z = 0 \quad \text{(ii)}$$

The value of E_z can be calculated as

$$E_z = \cos\left(\frac{m\pi x}{L}\right)\cos\left(\frac{n\pi y}{W}\right) \quad \text{(iii)}$$

Substituting the value of equation (iii) in equation (ii), and solving for k,

$$k^2 = \left(\frac{m\pi}{L}\right)^2 + \left(\frac{n\pi}{W}\right)^2 \quad \text{(iv)}$$

Since, $k = \omega\sqrt{\mu_0\varepsilon_0\varepsilon_r}$ (v)

and, $\omega = 2\pi f$ where f is the resonant frequency, thus f can be calculated as,

$$f = \frac{c}{2\pi\sqrt{\varepsilon_r}}\sqrt{\left(\frac{m\pi}{L}\right)^2 + \left(\frac{n\pi}{W}\right)^2} \quad \text{(vi)}$$

where $c = \frac{1}{\sqrt{\mu_0\varepsilon_0}}$ (vii)

For broadside beam radiation pattern, TM_{10} is usually used, Hence, for $m = 1$ and $n = 0$

$$E_z = \cos\left(\frac{\pi x}{L}\right) \quad \text{(viii)}$$

$$f_r = \frac{c}{2\sqrt{\varepsilon_r}}\left(\frac{1}{L}\right) \quad \text{(ix)}$$

From Figure 1,

$$L_{eff} = L + 2\Delta L \quad \text{(x)}$$

Hence, $f_r = \frac{c}{2\sqrt{\varepsilon_r}}\left(\frac{1}{L_{eff}}\right)$ (xi)

According to Hammerstad formula,

$$\Delta L = 0.412h\left[\frac{\left(E_{reff}+0.3\right)\left(\frac{W}{h}+0.264\right)}{\left(E_{reff}-0.258\right)\left(\frac{W}{h}+0.8\right)}\right] \quad \text{(xii)}$$

where, E_{reff} is the effective dielectric constant, h is the thickness of dielectric substrate, and W is the width of the patch. The value of E_{reff} can be calculated as

$$E_{reff} = \frac{\varepsilon_r + 1}{2} + \left(\frac{\varepsilon_r - 1}{2}\right)\left[1 + 12\left(\frac{h}{W}\right)\right]^{-1/2} \quad \text{(xiii)}$$

The width of the patch is given by

$$w = \frac{c}{2f_0\sqrt{\frac{(\varepsilon_r+1)}{2}}} \quad \text{(xiv)}$$

For sensible designs, some finite ground plane is essential beneath the substrate. For such practical design of microstrip patch antenna, it necessitate that the ground plane should be greater than the patch dimensions by approximately six times the substrate thickness [14-16]. Thus, the dimensions of the ground plane may be given as

$$L_g = 6h + l \quad \text{(xv)}$$

$$W_g = 6h + w \quad \text{(xvi)}$$

The input parameters of the microstrip patch antenna are estimated using above equations before finalizing the design for 3D modelling.

3. EXPERIMENTAL DESIGN

The proposed designed is simulated using FEM based computer simulation technology (CST MICROWAVE STUDIO) software in high frequency (HF) domain solver. Figure 2 shows the 3D geometry of the double layered slotted microstrip patch antenna design. It consists of two mirror L-slots on the square shaped patch. The dimensions of the designed antenna and location of the co-axial probe feed point is set using theoretical analysis as is given in the previous section. The operating range from single frequency to penta-frequency applications within the S-band depends on the distance and orientation of the slots as well as on the position of the probe feed point.

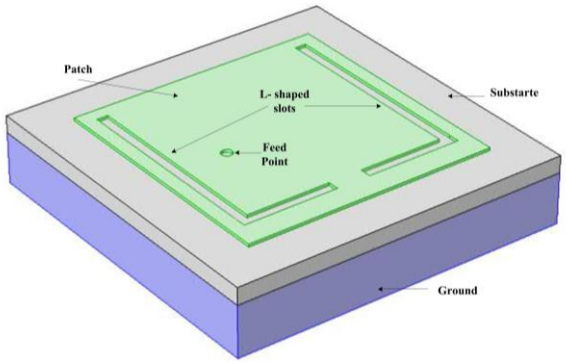

Fig. 2 – 3D Schematic of designed microstrip patch antenna

The top view of the double layered patch antenna is shown in Figure 3.

The proposed design is based on Roger's duroid RT-5880 substrate while the material selected for the patch is copper (Cu). The dimensions of the metallic patch are 45 × 45 mm^2 with thickness 0.5 mm. The thickness of the substrate is 3 mm. The designed antenna is enclosed in the square (90 × 90 mm^2) shaped domain with thickness 0.5 mm containing air or vacuum inside it. The domain is assumed to be surrounded by a perfectly matched layer (PML) so as to absorb the radiation from the antenna with minimum reflection, thus, contains minimum return loss. The dimensions of the bottom layer, i.e. ground are 60 mm × 60 mm × 9 mm. The material chosen for the ground and the patch are same. Table 1 shows the material properties that are equally accountable in simulating the design.

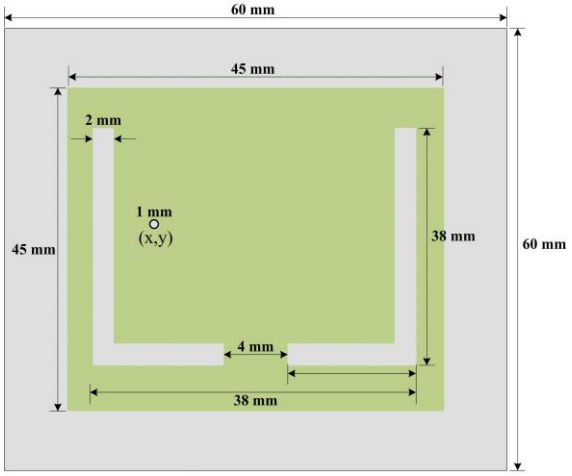

Fig. 3 – Top view of the design along with the dimensions

Table 1 – Material Properties

Properties	Materials		
	Rogers RT 5880	Copper (Cu)	Air in outer domain
Permittivity (ε_r)	2.2	1.0	1.0
Permeability (μ_r)	1.0	1.0	1.0
Density (kg/m^3)	2200	8700	1.16
Electrical conductivity (S/m)	0.001	60×10^6	0.00
Resistivity (Ωm)	2×10^{11}	1.72×10^{-8}	3.3×10^{16}

A coaxial probe feed point is selected in such a way that the proposed antenna design may work successfully for the number of operating frequency regions in the S-band. The position and the diameter of the coaxial probe influence the performance of the antenna. A multiband antenna is desirable if multiple narrow band channels are to be covered [17] [18]. The bandwidth of the antenna is directly proportional to the substrate thickness h. The impedance matching is difficult for higher value of h due to large probe inductance.

4. RESULTS AND DISCUSSIONS

The results verify the alteration in frequency bands and bandwidth with respect to change in position of the feed point.

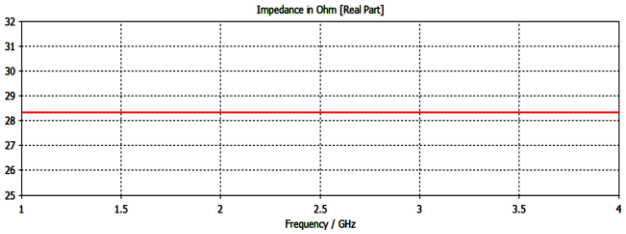

Fig. 4 – Characteristic impedance of the simulated antenna

Table 2 shows some of the selected coordinates of the feed point and their effect on performance parameters of the antenna. For this design simulation, the processing speed of the computational machine is 3.1 GHz with 4 GB RAM. The virtual memory used while simulation is 2.1 GHz. Precise sized meshing is not selected to avoid the computational load. Frequency domain setting is selected for simulating the model. The characteristic impedance (Z_0) of the simulated design comes out to be 28.3 Ω and is shown in Figure 4. Theoretically, the value of Z_0 is 50 Ω that shows small existence of standing waves while propagation of RF signals. Some of the simulated results are shown in Figures 5-8. We have simulated the results for each usable frequency while altering the position of coaxial feed point and found that the results are noticeably different with the changing position of feed point. Figure 7 shows the far field gain for the feed point coordinate (– 9,0) and the far field gain is obtained for five different frequencies with maximum gain varying between – 6.1 dBM/m^2 to – 3.91 dBM/m^2.

Similarly, Fig. 8 shows the far filed gain while changing the feed point co-ordinates from (– 9,0) to (– 5,0).

Table 2 – Parametric variations with respect to change in feed point position

Feed point (x, y)	Resonant frequencies (GHz)	Return Losses S11	Bandwidth (MHz)	Gain (dB)	E-field (dB)	H-field (dB)	Power (dB)
– 15, – 15	2.7640	– 10.73	11.6	6.013	20.40	– 31.12	– 5.361
– 5,0	2.1820	– 24.00	38.0	7.097	21.85	– 29.67	– 3.912
	2.7544	– 15.78	31.0	6.104	20.76	– 30.76	– 5.004
– 7,0	2.182	– 32.45	37.4	7.098	21.86	– 29.66	– 3.897
	2.7725	– 19.07	45.0	6.024	20.74	– 30.78	– 5.022
	3.162	– 25.15	57.0	5.265	20.02	– 31.50	– 5.740
– 8,0	2.182	– 38.26	37	7.095	21.86	– 29.66	– 3.898
	2.7831	– 13.98	40	5.990	20.58	– 30.94	– 5.180
	3.1719	– 24.21	70	5.354	20.11	– 31.42	– 5.655
	3.6484	– 11.54	20	6.047	20.50	– 31.02	– 5.261
– 9,0	1.6449	– 12.76	36.0	5.553	20.09	– 31.43	– 6.101
	2.1820	– 28.79	35.0	7.088,	21.85	– 29.67	– 3.910
	2.7900	– 11.57	30.0	5.920,	20.37	– 31.16	– 5.395
	3.1800	– 16.00	68.4	5.442,	20.09	– 31.43	– 5.667
	3.6500	– 14.79	30.0	6.008	20.63	– 30.89	– 5.131

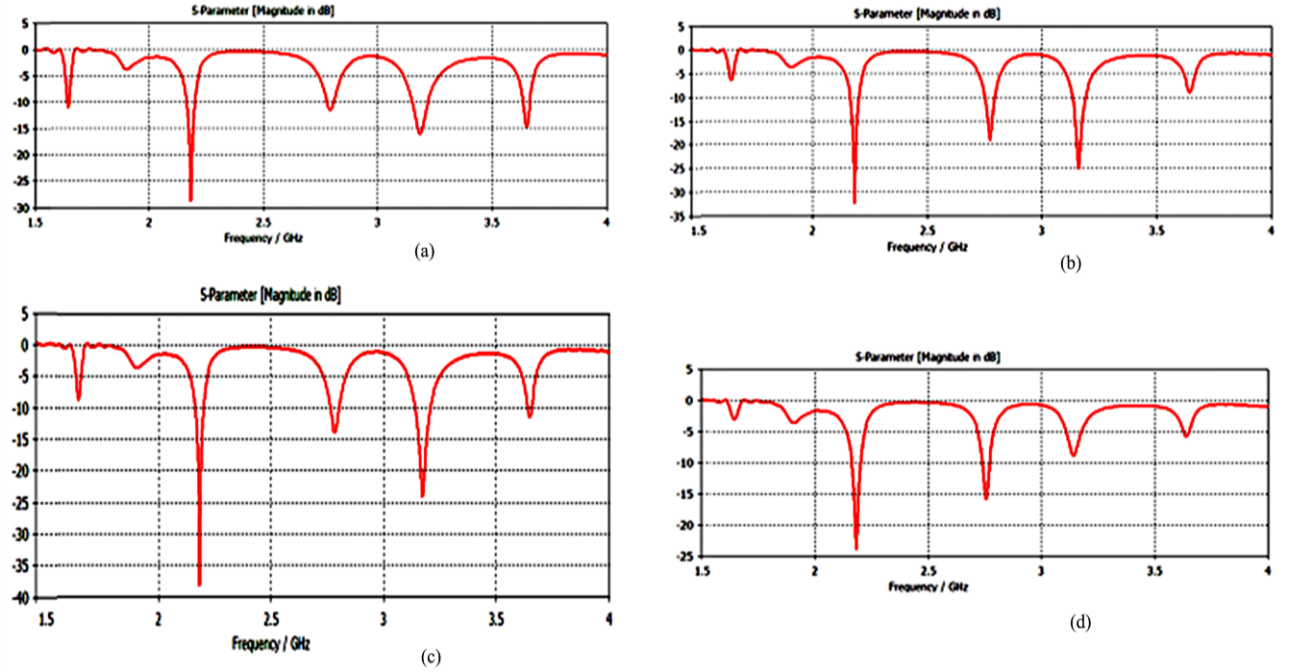

Fig. 5 – Graphs showing s-parameters values for different coaxial positions: (a) (– 9,0), (b) (– 7,0), (c) (– 8,0) and (d) (– 5,0)

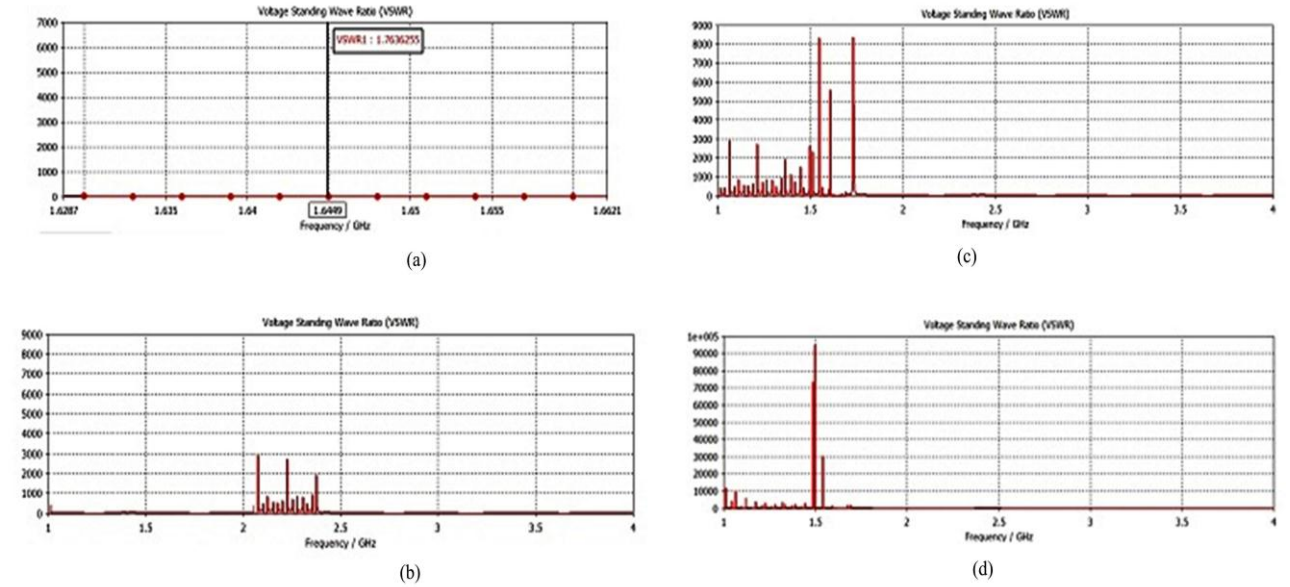

Fig. 6 – Graphs showing VSWR values for coaxial positions: (a) (– 9,0), (b) (– 7,0), (c) (– 8,0) and (d) (– 5,0)

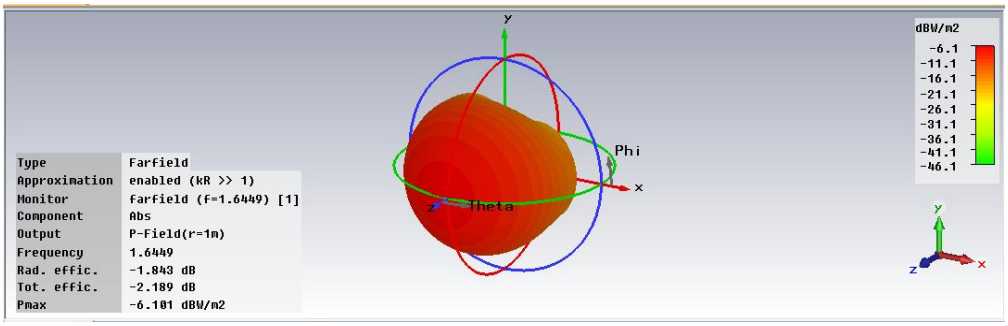

a

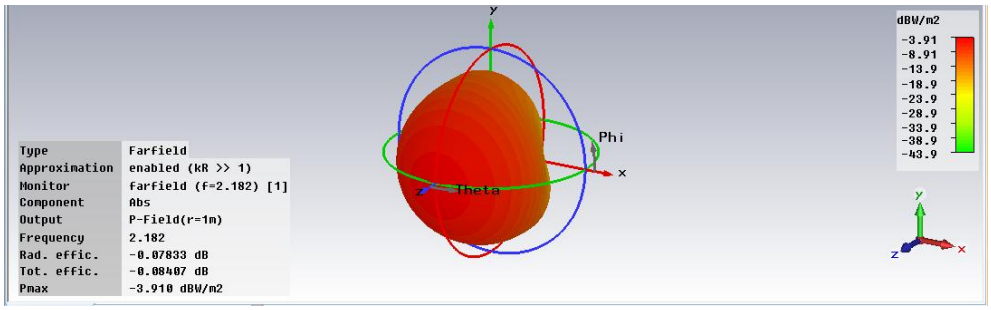

b

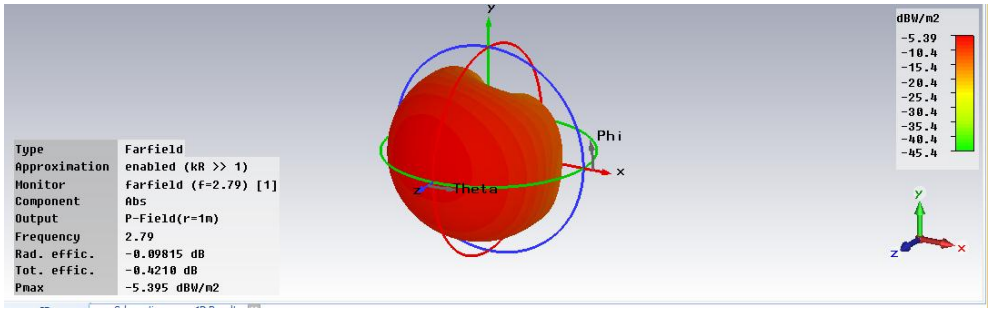

c

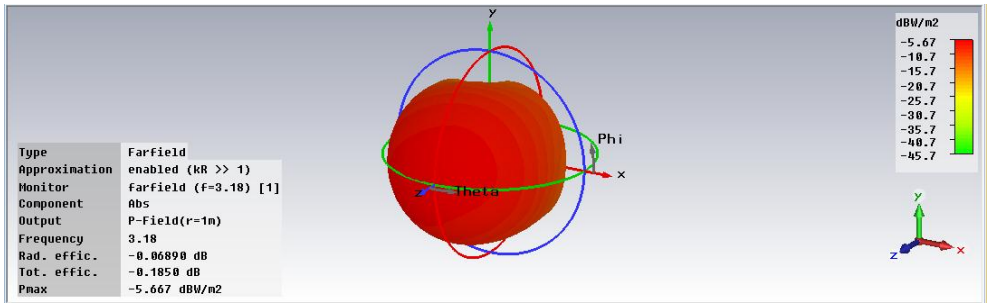

d

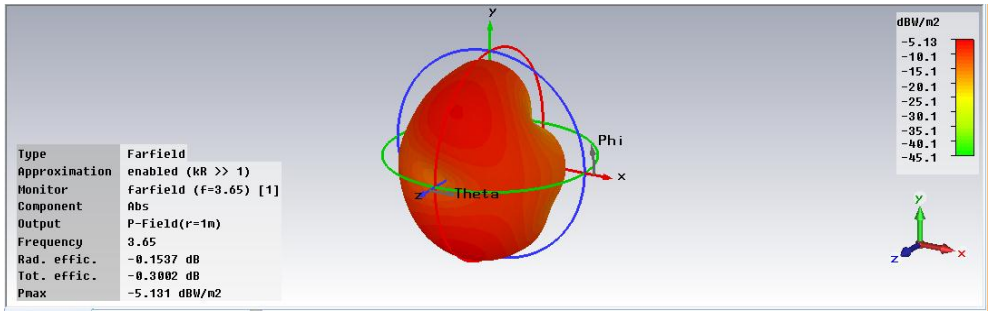

e

Fig. 7 – Far field radiation pattern for coaxial position (– 9,0) at different resonant frequencies: (a) 1.6449 GHz, (b) 2.182 GHz, (c) 2.79 GHz, (d) 3.18 GHz, and (e) 3.65 GHz

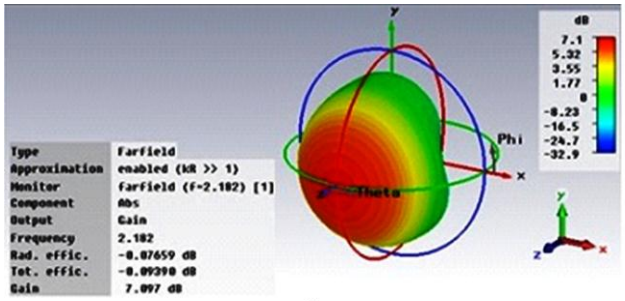

(a)

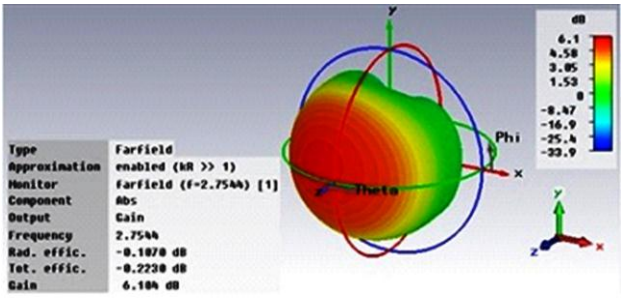

(b)

Fig. 8 – Far field radiation pattern for coaxial position (– 5,0) at resonant frequencies: (a) 2.182 GHz, and (b) 2.7544 GHz

The electric field distribution characteristics indicate that all the resonant modes for different coaxial positions can be tuned and controlled independently. Results show that despite a small distortion, the radiation patterns are reasonably well enough to work in different frequency bands. This feature of varying coaxial point is attractive for the designed antenna where multi-frequencies can be handled with satisfactory gain and radiation patterns. The value of E- and H-plane field is also shown in Table 2. The antenna can be operated well between frequency ranges 1.6449 GHz to 3.6484 GHz with good bandwidth. Hence the frequency diversity is verified with good performance of the antenna.

5. CONCLUSION

In the present work, a multi-frequency microstrip patch antenna is designed by using coaxial probe feed. Two *L*-slots are used to design a single, dual, triple, quad and a penta-band antenna. This design does not require complex circuitry and is based on mono layer, single patch. The gain of antenna is high enough, having 5.354 dB smaller value of gain. The characteristic impedance (28.3 Ω) is low but the impedance matching is accurate. The proposed antenna can handle mutliple frequencies by simply varying the feed point and covers lot of demanding frequency slots used in day-to-day communication systems.

ACKNOWLEDGEMENT

The first author wishes to thank the University Grants Commission (UGC), India for providing financial assistance to complete this work in the form of minor research project.

REFERENCES

1. A. Elsherbini, K. Sarabandi, *IEEE Antennas Wireless Propag. Lett.* **10**, 75 (2011).
2. Y. Cao, B. Yuan, G. Wang, *IEEE Antennas Wireless Propag. Lett.* **10**, 911 (2011).
3. D.M. Pozar, D.H. Schaubert, *Microstrip Antennas: The analysis and design of microstrip antennas and arrays* (Wiley: IEEE Press: 1995).
4. K.L. Wong, *Compact and broadband microstrip antennas* (John Wiley: 2003).
5. G. Kumar, K.P. Ray, *Broadband microstrip antennas* (Artech House: 2002).
6. A.A. Deshmukh, K.P. Ray, *IEEE Antennas Propag. Magazine* **53**, 41 (2011).
7. C.I. Lin, K.L. Wong, *IEEE T. Antennas Propag.* **55**, 3690 (2007).
8. S. Weigand, G.H. Huff, K.H. Pan, J.T. Bernhard, *IEEE T. Antennas Propag.* **51**, 457 (2003).
9. W.C. Mok, S.H. Wong, K.M. Luk, K.F. Lee, *IEEE T. Antennas* **61**, 4341 (2013).
10. J. Anguera, G. Font, C. Puente, C. Borja, J. Soler, *IEEE Microwave Wireless Component. Lett.* **13**, 123 (2003).
11. S. Arya, S. Khan, C. Shan, P. Lehana, *J. Computational Intellig. Electron. System.* **1**, 178 (2012).
12. R. Arora, A. Kumar, S. Khan, S. Arya, *Int. J. Commun. Antenna Propag.* **4**, 27 (2014).
13. Z. Safa, Z. Lahbib, *J. Microwave., Optoelectron. Electromagn. Appl.* **12**, 23 (2013).
14. F. Croq, D.M. Pozar, *IEEE T. Antennas Propag.* **40**, 1367 (1992).
15. T. Huynh, K.F. Lee, *Electron Lett.* **31**, 1310 (1986).
16. F. Yang, X.X. Zhang, X. Ye, Y. Rahmat-Samii, *IEEE T. Antennas Propag.* **49**, 1094 (2001).
17. K.O. Odeyemi, D.O. Akande, E.O. Ogunti, *Eur. J. Sci. Res.* **55**, 72 (2011).
18. K.F. Lee, S.L.S. Yang, A. Kishk, *IEEE Antennas Wireless Commun. Lett.* **7**, 645 (2008).